# Protocol Dependence of the Jamming Transition

Thibault Bertrand,[1] Robert P. Behringer,[2] Bulbul Chakraborty,[3] Corey S. O'Hern,[1,4,5] and Mark D. Shattuck[6,1]

[1]*Department of Mechanical Engineering and Materials Science, Yale University, New Haven, Connecticut, 06520, USA*
[2]*Department of Physics and Center for Nonlinear and Complex Systems, Duke University, Durham, North Carolina, 27708-0305, USA*
[3]*Martin Fisher School of Physics, Brandeis University, Mail Stop 057, Waltham, Massachusetts, 02454-9110, USA*
[4]*Department of Physics, Yale University, New Haven, Connecticut, 06520, USA*
[5]*Department of Applied Physics, Yale University, New Haven, Connecticut, 06520, USA*
[6]*Department of Physics and Benjamin Levich Institute, The City College of the City University of New York, New York, 10031, USA*

(Dated: June 17, 2015)

We propose a theoretical framework for predicting the protocol dependence of the jamming transition for frictionless spherical particles that interact via purely repulsive contact forces. We study isostatic jammed disk packings obtained via two protocols: isotropic compression and simple shear. We show that for frictionless systems, all jammed packings can be obtained via either protocol. However, the probability to obtain a particular jammed packing depends on the packing-generation protocol. We predict the average shear strain required to induce jamming in initially unjammed packings from the measured probability to jam at packing fraction $\phi$ from isotropic compression. We compare our predictions to results from numerical simulations of jamming and find quantitative agreement. We also show that the packing fraction range, over which strain-induced jamming occurs, tends to zero in the large system limit for frictionless packings with overdamped dynamics.

PACS numbers: 45.70.-n,61.43.-j,64.70.ps,83.80.Fg

Dry granular materials are composed of macro-sized particles that interact via purely repulsive forces. Due to strongly dissipative interactions between grains, granular materials exist as mechanically stable, static packings in the absence of externally imposed driving forces [1]. As a consequence, granular packings are strongly out-of-equilibrium, and thus their structural and mechanical properties depend on the protocol that was used to generate them. Common experimental packing-generation protocols include gravitational deposition [2], vibration [3], compression [4], and shear [5, 6]. Several computational studies have pointed out that the distribution of jammed packing fractions depends on the compression rate [7, 8] and rate at which kinetic energy is removed from the system [9, 10]. In addition, experimental studies of photoelastic disks have identified key differences between static granular packings that are generated via isotropic compression and pure shear [11].

There has been a significant amount of work on understanding the scaling behavior of the elastic moduli and contact number near the onset of jamming in model granular packings composed of frictionless spherical particles generated using isotropic compression [12]. However, there is currently no theoretical understanding of how the ensemble of static packings and their properties vary with the protocol that was used to generate them. For example, what is the difference in the distribution of jammed packings generated via isotropic compression versus shear?

In this Letter, we focus on isostatic jammed packings of frictionless disks generated via different combinations of isotropic compression and simple shear strain and study the distribution of jammed packings as a function of the particular path taken through configuration space. We find several important results. First, an exponentially large but finite number of jammed packings with an isostatic number of contacts $N_c = N_c^{\rm iso} = 2N' - 1$ (where $N'$ is the number of disks in the force-bearing backbone) exist in configuration space, defined by the positions of the disks, packing fraction $\phi$, and shear strain deformation $\gamma$ of the system boundaries. In small systems, nearly all of the jammed packings in configuration space can be enumerated [13]. For example, we have shown that isostatic jammed packings form one-dimensional geometrical families as a function of shear strain [14]. We will show that the choice of the packing-generation protocol does not change the full ensemble of isostatic, jammed packings, but instead changes which of the packings are visited during particular trajectories through configuration space. The average properties of jammed packings change for different protocols because the probabilities for obtaining each of the jammed packings varies with the packing-generation protocol.

We develop a theoretical description of the protocol dependence of the distribution of jammed disk packings (Fig. 1). We assume that an initially unjammed system will jam when it encounters the basin of attraction of a jammed packing as it travels through configuration space. The probability to obtain a jammed packing is thus determined by two factors: 1) the density of jammed packings in configuration space, which is independent of the packing protocol, and 2) the path traveled through configuration space, which depends explicitly on the protocol. Using this framework, we predict the average shear strain

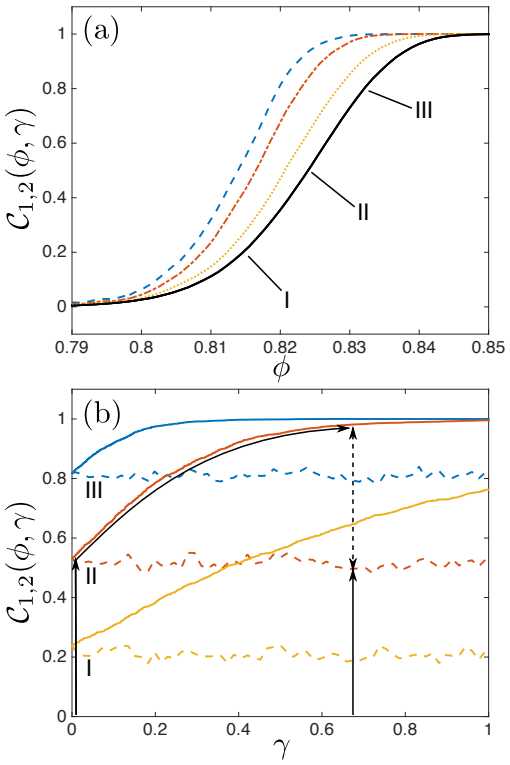


FIG. 1: Fraction of jammed packings (or cumulative distribution) $\mathcal{C}(\phi,\gamma)$ along different paths in the packing fraction $\phi$ and shear strain $\gamma$ plane for $N = 32$. (a) $\mathcal{C}_1(\phi,\gamma)$ for protocol 1 (isotropic compression at fixed $\gamma$; solid line) and $\mathcal{C}_2(\phi,\gamma)$ for protocol 2, *i.e.* compression to packing fraction $\phi$ followed by applied shear strain to $\gamma = 0.1$ (dotted line), 0.3 (dot-dashed line), and 0.5 (dashed line). I, II, and III indicate the packing fractions displayed in panel (b). (b) We show $\mathcal{C}_1(\phi,\gamma)$ (dashed lines) and $\mathcal{C}_2(\phi,\gamma)$ (solid lines) at fixed packing fractions $\phi = 0.815$, 0.824, and 0.832 indicated by I-III. Protocol dependence can be seen in the difference between $\mathcal{C}_1$ and $\mathcal{C}_2$ evaluated at the same $\phi$ and $\gamma$, *e.g.* at $\phi = 0.824$ and $\gamma = 0.67$ as highlighted by the dashed double arrow. The right and left solid arrows indicate protocols 1 and 2, respectively.

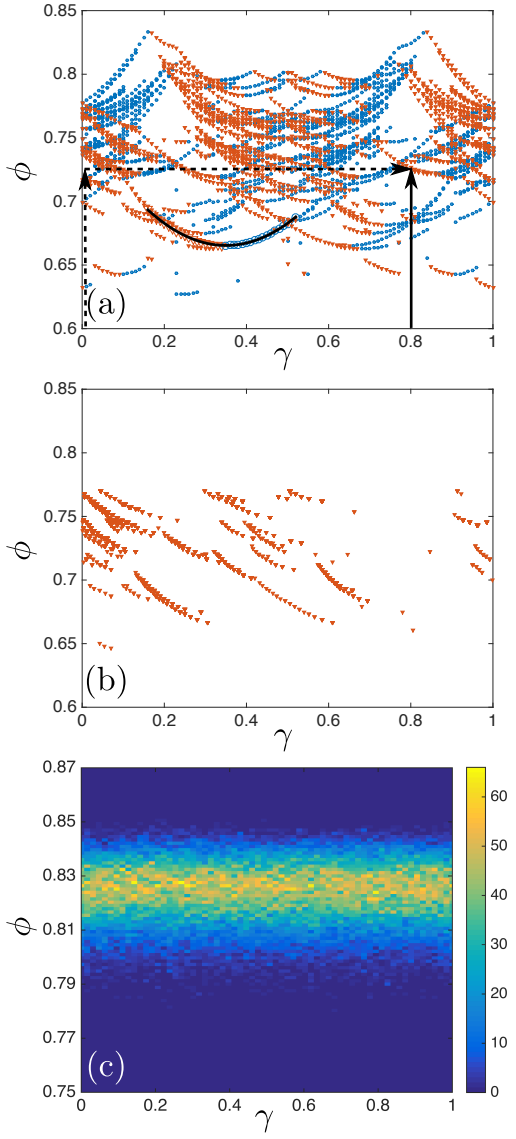


FIG. 2: (a) Packing fraction $\phi$ versus shear strain $\gamma$ for all jammed $N = 6$ disk packings. The solid black line obeys $\phi = A(\gamma - \gamma_0)^2 + \phi_0$ with $A = 0.776$, $\phi_0 = 0.665$, and $\gamma_0 = 0.35$. The filled circles (downward triangles) indicate packings with positive (negative) local slope. The solid vertical arrow indicates protocol 1 (isotropic compression at fixed boundary shape), and the dashed vertical arrow followed by the dashed horizontal arrow indicate protocol 2 that was used to reach a particular jammed packing at $\gamma = 0.8$ and $\phi = 0.725$. (b) Jammed packing fraction $\phi(\gamma)$ using protocol 2 at fixed packing fraction in the range $0.64 < \phi < 0.77$ for $N = 6$. (c) Number of $N = 32$ jammed packings with packing fraction $\phi$ and shear strain $\gamma$ (on a linear scale increasing from dark to light) generated using protocol 1.

required for unjammed packings to jam at each $\phi$ and show that the predictions agree with simulations of shear strain-induced jamming. Our results indicate that the packing fraction range, over which shear strain-induced jamming occurs, vanishes in the large-system limit for overdamped frictionless systems.

We study systems containing $N$ frictionless bidisperse disks in a parallelogram with constant height $L = 1$ in two dimensions that interact via purely repulsive linear spring forces with characteristic energy scale $\epsilon$ [15]. The bidisperse mixtures are composed of half large and half small particles with mass $m = 1$ for both and diameter ratio $\sigma_L/\sigma_S = 1.4$. We employ Lees-Edwards simple shear-periodic boundary conditions, where the top (bottom) images of the central simulation cell are shifted to the right (left) by shear strain $\pm\gamma$ [16]. We varied the system size from $N = 6$ to 512 disks.

Below, we describe results for several protocols to generate mechanically stable packings in the packing fraction $\phi$ and shear strain deformation $\gamma$ plane. (See Fig. 2 (a).) Protocol 1 involves isotropic compression at fixed boundary shape parametrized by the shear strain $\gamma$. We start

with random initial disk positions at $\phi_0 = 0.5$ [17]. We successively compress the system by increasing the particle radii uniformly in small packing fraction increments $d\phi$ and minimize the total potential energy per particle $V/(N\epsilon)$ (at fixed $\gamma$) after each compression step. The onset of jamming occurs when $10^{-16} > V/(N\epsilon) > 0$. For protocol 2, we start by isotropically compressing systems (at $\gamma = 0$) to packing fraction $\phi$, and if the system is unjammed with $V/(N\epsilon) = 0$, we successively apply simple shear strain to each particle $x_i' = x_i + d\gamma y_i$ in strain steps $d\gamma < 10^{-3}$ followed by minimization of $V/(N\epsilon)$ after each strain step. We then identify the total shear strain $\gamma$ at which the system first jams with $10^{-16} > V/(N\epsilon) > 0$.

We display the results for the cumulative distributions $\mathcal{C}_{1,2}(\phi, \gamma)$ of jammed packings from the two protocols in Fig. 1. In (a), we show that applying shear strain increases the fraction of jammed packings at each $\phi$, *i.e.* $\mathcal{C}_2(\gamma, \phi)$ shifts to lower $\phi$ with increasing $\gamma$. In (b), we show $\mathcal{C}_1(\phi, \gamma)$ obtained via isotropic compression as a function of the boundary shape for three packing fractions $\phi = 0.815$, 0.824, and 0.832 (corresponding to $\mathcal{C}_1(\phi, 0) \approx 0.2$, 0.5, and 0.8). In (b), $1 - \mathcal{C}_1(\phi, 0)$ of the packings are initially unjammed at $\gamma = 0$ and $\phi$, and these initially unjammed packings tend to jam with increasing shear strain as shown by the solid lines. By combining different amounts of shear strain and isotropic compression, the fraction of jammed packings at a given $\phi$ can be tuned over a wide range, *e.g.* from 0.2 to 0.8 for packings at $\phi = 0.815$. These results emphasize that the distribution of jammed packings depends strongly on the particular path taken through configuration space, *e.g.* protocols 1 and 2 indicated by the arrows in Fig. 1 (b).

To understand this protocol dependence, we examine the distribution of jammed packings in the $\phi$-$\gamma$ plane. In Fig. 2 (a), we show the packing fraction at jamming onset $\phi$ versus shear strain $\gamma$ for $N = 6$ obtained from protocol 1 (trajectory given by the solid vertical arrow in Fig. 2 (a)). We find several striking features. First, jammed packings occur as geometrical families (*i.e.* segments of parabolas that correspond to jammed packings with the same interparticle contact network) in the $\phi$-$\gamma$ plane. For $N = 6$, we are able to enumerate nearly all of the geometrical families over the full range of $\gamma$ [14]. When straining an initially unjammed system toward positive $\gamma$ at fixed $\phi$ (*e.g.* the horizontal arrow in Fig. 2 (a)), it will jam on a geometrical family with negative slope $(-|d\phi/d\gamma|)$. For negative slopes, continued shear strain leads to overcompression, whereas for positive slopes, continued shear strain leads to unjamming. This behavior is shown explicitly in Fig. 2 (b) for the shear strain protocol at fixed packing fraction in the range $0.64 < \phi < 0.77$ for $N = 6$. Note that any of the jammed packings in Fig. 2 (b) obtained using the shear strain protocol and defined by $\{\vec{r}_i\}$, $\phi$, and $\gamma$ can be generated using the isotropic compression protocol with initial condition $\{\vec{r}_i\}$ and boundary deformation $\gamma$. As a result, we can generate the same jammed packing at a given $\phi$ and $\gamma$ using different combinations of compression and shear strain. We find similar

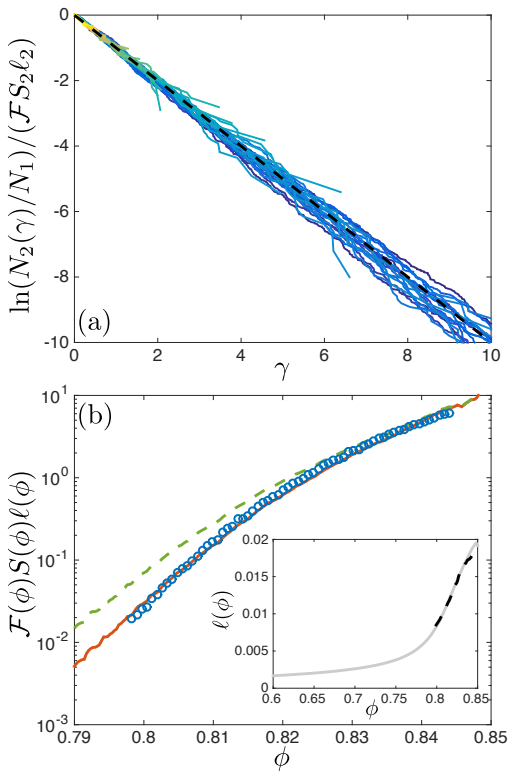


FIG. 3: (a) Natural logarithm of the fraction of unjammed packings (normalized by the $\phi$-dependent decay factor, $\mathcal{F}(\phi)S_2(\phi)\ell_2(\phi)$), during the shear-strain protocol at fixed packing fraction in the range $0.798 < \phi < 0.844$ (solid lines) for $N = 32$. The dashed line has slope $-1$. (b) A comparison of $-d\ln[N_2(\phi,\gamma)/N_0]/d\gamma$ (open circles) from protocol 2 and $-d\ln[N_1(\phi)/N_0]/d\phi$ from protocol 1 with $S_2(\phi) \propto S_1(\phi)\ell_1(\phi)$ (solid line) or $S_2(\phi) \propto S_1(\phi)$ (dashed line) for $N = 32$. The inset of (b) shows the distances $\ell_1(\phi)$ and $\alpha\ell_2(\phi)$ (with $\alpha \approx 5.5$) traversed in configuration space during protocols 1 (solid line) and 2 (dashed line) for $N = 32$.

behavior to that in Fig. 2 (a) and (b) for larger $N$, except that the parabolic segments in $\phi(\gamma)$ become smaller and more numerous, and thus geometrical families more densely populate configuration space (Fig. 2 (c)). We find that the number of jammed packings at a given $\phi$ and $\gamma$ becomes independent of $\gamma$ for system sizes $N \geq 32$.

Based on these results, we develop a theoretical model using an analogy with absorption problems to calculate the probability to obtain isostatic jammed packings as a function of the path that the system traverses in configuration space. We assume that the density of jammed packings $\mathcal{F}(\phi)$, defined in the $2N$-dimensional configuration space, only depends on the packing fraction $\phi$, and not on the packing-generation protocol. We imagine that a one-dimensional trajectory $\mathcal{L}(\phi, \gamma)$ through configuration space will encounter the basin of attraction [18] of a jammed packing with a probability of $\mathcal{F}(\phi)S(\phi)d\mathcal{L}$ during a step of size $d\mathcal{L}$ in configuration space, where $S(\phi)$ is the average $2N-1$-dimensional cross-section of the

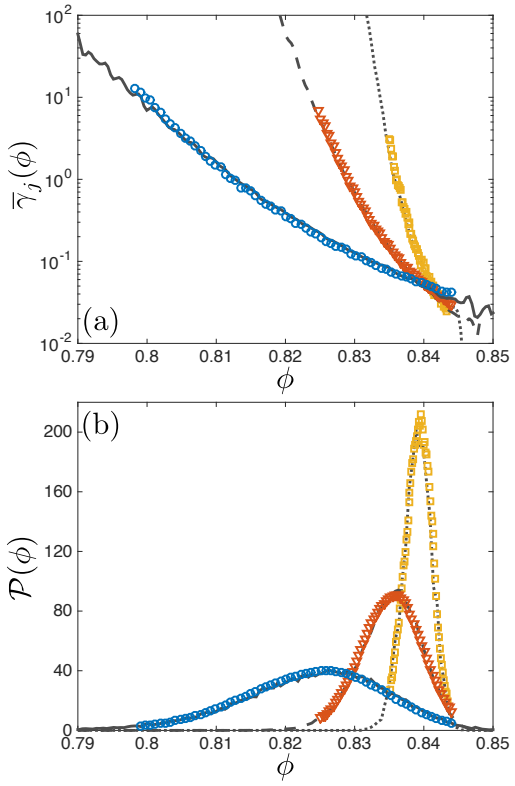


FIG. 4: (a) Average shear strain $\overline{\gamma}_j(\phi)$ necessary to jam an initially unjammed configuration at $\phi$ and $\gamma = 0$ obtained from simulations of successive applications of simple shear strain followed by energy minimization for $N = 32$ (circles), 128 (triangles), and 512 (squares). We compare $\overline{\gamma}_j(\phi)$ from protocol 2 to $1/(\mathcal{F}(\phi)S_1(\phi)\ell_1^2(\phi))$ (Eqs. 3 and 4) obtained from isotropic compression (protocol 1) for the same system sizes: $N = 32$ (solid line), 128 (dashed line), and 512 (dotted line). (b) Distribution of jammed packing fractions $\mathcal{P}_1(\phi)$ obtained from simulations of isotropic compression for $N = 32$ (solid line), 128 (dashed line), and 512 (dotted line) compared to predictions obtained from $\mathcal{P}_1(\phi) = -N_0^{-1}dN_1(\phi)/d\phi$ with $N_1(\phi)$ given by Eq. 2 and $\mathcal{F}(\phi)S_1(\phi)l_1(\phi)$ given by Eq. 4 using the measured value of $\overline{\gamma}_j$ for the same system sizes: $N = 32$ (circles), 128 (triangles), and 512 (squares).

basin of attraction of a jammed packing perpendicular to $d\mathcal{L}$. Thus, for protocol 1 with trajectories only along $\phi$ in configuration space, the decrease in the number of unjammed packings $dN_1(\phi)$ (or equivalently an increase in the number of jammed packings) during a compression step $d\phi$ is given by

$$dN_1(\phi) = -N_1(\phi)\mathcal{F}(\phi)S_1(\phi)\ell_1(\phi)d\phi, \qquad (1)$$

where $\ell_1(\phi)$ is the distance in configuration space traversed during the step $d\phi$ at packing fraction $\phi$ and $S_1(\phi)$ is the average cross section for protocol 1. This differential equation can be solved for the number of unjammed packings at $\phi$ during compression:

$$N_1(\phi) = N_0 \exp\left[-\int_{\phi_0}^{\phi} \mathcal{F}(\phi')S_1(\phi')\ell_1(\phi')d\phi'\right], \qquad (2)$$

where $N_0$ is the number of unjammed packings at $\phi_0$. For protocol 2 with trajectories that move along $\gamma$ in configuration space, we obtain a similar expression for the number of unjammed packings: $dN_2(\phi,\gamma)/d\gamma = -N_2(\phi,\gamma)\mathcal{F}(\phi)S_2(\phi)\ell_2(\phi)$, where $N_2(\phi,\gamma) = N_1(\phi)\exp[-\mathcal{F}(\phi)S_2(\phi)\ell_2(\phi)\gamma]$, $S_2(\phi)$ is the average cross section for protocol 2, and $\ell_2(\phi)$ is the distance traversed in configuration space for each shear strain step $d\gamma$.

Fig. 3 (a) shows that the fraction of unjammed packings $N_2(\phi,\gamma)/N_1(\phi)$ decays exponentially with $\gamma$ during protocol 2 at each fixed $\phi$ and provides excellent support for the absorption description of jamming. In the zeroth order approximation, the average cross section $S(\phi)$ is independent of the path taken in configuration space and the distance $\ell$ traveled during each $d\phi$ or $d\gamma$ step is constant. In Fig. 3 (b), we compare $\mathcal{F}(\phi)S(\phi)\ell$ obtained from protocol 2 with the similar quantity $-d\ln[N_1(\phi)/N_0]/d\phi$ from protocol 1 and find qualitative agreement.

We then independently measured $\ell_1(\phi)$, defined by the accumulated distance in configuration space between the initial packing at $\phi$ and the relaxed packing at $\phi + d\phi$, for the compression protocol. We performed similar measurements for $l_2(\phi)$, which gives the accumulated distance in configuration space between the initial packing at $\gamma$ and the relaxed packing at $\gamma + d\gamma$ for protocol 2. We show that the two distances are proportional to each other, $\ell_1(\phi) = \alpha\ell_2(\phi)$ with $\alpha \approx 5.5$, in the inset of Fig. 3 (b). Then, by calculating $-d\ln[N_1(\phi)/N_0]/d\phi = \mathcal{F}(\phi)S_1(\phi)\ell_1(\phi)$ for protocol 1 (isotropic compression), we can compare $\mathcal{F}(\phi)S_1(\phi)\ell_1(\phi)$ to the similar quantity, $\mathcal{F}(\phi)S_2(\phi)\ell_2(\phi)$, for protocol 2 (shear strain). In this case, we assume that the average cross section depends on the path taken in configuration space, *e.g* isotropic compression increases the overlap of all interparticle contacts, while applied shear strain increases some but decreases others. In Fig. 3 (b), we show excellent agreement for $\mathcal{F}(\phi)S_{1,2}(\phi)\ell_{1,2}(\phi)$ for protocols 1 and 2 for $N = 32$ provided we assume that $S_2(\phi) \propto S_1(\phi)\ell_1(\phi)$, and we find similar quantitative agreement for all system sizes studied. Independent measurements of $S_{1,2}(\phi)$ will be performed in future studies.

We can now use the theoretical description of the protocol-dependent probability to jam to predict the average shear strain required to jam an initially unjammed isotropically compressed configuration at $\phi$ and $\gamma = 0$:

$$\overline{\gamma}_j(\phi) = \int_0^{\infty} \gamma \frac{N_2(\phi,\gamma)}{N_1(\phi)}d\gamma = \frac{1}{\mathcal{F}(\phi)S_2(\phi)\ell_2(\phi)} \qquad (3)$$

$$\simeq \frac{\alpha}{\mathcal{F}(\phi)S_1(\phi)\ell_1^2(\phi)}. \qquad (4)$$

In Fig. 4 (a), we show that the theoretical prediction for $\overline{\gamma}_j(\phi)$, obtained from measurements of $\mathcal{F}(\phi)S_1(\phi)\ell_1^2(\phi)$

using isotropic compression, agrees with the results from simulations of shear strain-induced jamming. We find that the average shear strain $\overline{\gamma}_j$ required to jam an initially unjammed configuration grows rapidly with increasing system size and that only packings with $\phi \gtrsim 0.84$ are jammed in the large-system limit [19]. We are also able to calculate the distribution $\mathcal{P}_1(\phi)$ of jammed packing fractions (for isotropic compression) using the data from shear strain protocol. In Fig. 4 (b), we show that $\mathcal{P}_1(\phi)$ obtained from simulations of isotropic compression and $\mathcal{P}_1(\phi) = -N_0^{-1} dN(\phi)/d\phi$ with $N_1(\phi)$ given by Eq. 2 and $\mathcal{F}(\phi)S_1(\phi)\ell_1(\phi)$ given by Eq. 4 (using the measured value of $\overline{\gamma}_j$) collapse for all system sizes studied. The width of $\mathcal{P}_1(\phi)$ for isotropic compression narrows as $1/N^\alpha$ with $\alpha \approx 0.55 \pm 0.05$ and the peak in the distribution approaches $\phi_{\rm rcp} \approx 0.842$ in the large-system limit [19].

In this manuscript, we developed a theoretical description for the onset of jamming that allows us to predict the fraction of isostatic jammed packings that occur at a given packing fraction $\phi$ and shear strain $\gamma$ in terms of the path that is traversed in configuration space. This framework provides predictions for the average shear-strain required to induce jamming in initially unjammed packings produced by isotropic compression, which agree quantitatively with overdamped simulations of strain-induced jamming. In particular, we show that the packing fraction range, over which strain-induced jamming occurs, shrinks to zero in the large-system limit for frictionless systems with overdamped dynamics. In future studies, we will investigate the role of static friction in stabilizing strain-induced jamming of dilute granular packings [5].

### Acknowledgments

We acknowledge financial support from the Army Research Office Grant No. W911NF-14-1-0005 (T.B.), W. M. Keck Foundation Grant No. DT061314 (T.B., R.B., B.C., and C.S.O.), and the National Science Foundation (NSF) Grant Nos. CBET-0968013 (M.D.S.) and DMR-1409093 (B.C.). We also acknowledge support from the Kavli Institute for Theoretical Physics (through NSF Grant No. PHY-1125915), where some of this work was performed. This work benefited from the facilities and staff of the Yale University Faculty of Arts and Sciences High Performance Computing Center and the NSF (Grant No. CNS-0821132) that in part funded acquisition of the computational facilities.

[1] H. M. Jaeger, S. R. Nagel, and R. P. Behringer, *Rev. Mod. Phys.* **68** (1996) 1259.
[2] G. Y. Onoda and E. G. Liniger, *Phys. Rev. Lett.* **64** (1990) 2727.
[3] W. R. Nowak, J. B. Knight, E. Ben-Naim, H. M. Jaeger, and S. R. Nagel, *Phys. Rev. E* **57** (1998) 1971.
[4] T. S. Majmudar, M. Sperl, S. Luding, and R. P. Behringer, *Phys. Rev. Lett.* **98** (2007) 058001.
[5] D. Bi, J. Zhang, B. Chakraborty, and R. P. Behringer, *Nature* **480** (2011) 355.
[6] N. Kumar and S. Luding, arXiv:1407.6167.
[7] S. Torquato, T. M. Truskett, and P. G. Debenedetti, *Phys. Rev. Lett.* **84** (2000) 2064.
[8] K. Zhang, W. W. Smith, M. Wang, Y. Liu, J. Schroers, M. D. Shattuck, and C. S. O'Hern, *Phys. Rev. E* **90** (2014) 032311.
[9] P. Chaudhuri, L. Berthier, and S. Sastry, *Phys. Rev. Lett.* **104** (2010) 165701.
[10] C. F. Schreck, C. S. O'Hern, and L. E. Silbert, *Phys. Rev. E* **84** (2011) 011305.
[11] T. S. Majmudar and R. P. Behringer, *Nature* **435** (2005) 1079.
[12] A. J. Liu and S. R. Nagel, *Ann. Rev. Condens. Matter Phys.* **1** (2010) 347.
[13] G.-J. Gao, J. Blawzdziewicz, C. S. O'Hern, and M. D. Shattuck, *Phys. Rev. E* **80** (2009) 061304.
[14] G.-J. Gao, J. Blawzdziewicz, and C. S. O'Hern, *Phys. Rev. E* **80** (2009) 061303.
[15] C. S. O'Hern, L. E. Silbert, A. J. Liu, and S. R. Nagel, *Phys. Rev. E* **68** (2003) 011306.
[16] A. W. Lees and S. F. Edwards, *J. Phys. C Solid State* **5** (1972) 1921.
[17] Our results do not depend on the initial packing fraction for $\phi_0 \leq 0.5$.
[18] S. S. Ashwin, J. Blawzdziewicz, C. S. O'Hern, and M. D. Shattuck, *Phys. Rev. E* **85** (2012) 061307.
[19] N. Xu, J. Blawzdziewicz, and C. S. O'Hern, *Phys. Rev. E* **71** (2005) 061306.